Liquid xenon as an ideal probe for many-body effects in impulsive Raman scattering

Boeijenga, N. H.; Pugzlys, A.; la Cour Jansen, T.; Snijders, J. G.; Duppen, K.

Published in:
Journal of Chemical Physics

DOI:
10.1063/1.1483862

Publication date:
2002

Liquid xenon as an ideal probe for many-body effects in impulsive Raman scattering

Nienke H. Boeijenga, Audrius Pugzlys, Thomas l. C. Jansen, Jaap G. Snijders, and Koos Duppen

Citation: J. Chem. Phys. **117**, 1181 (2002); doi: 10.1063/1.1483862
View online: https://doi.org/10.1063/1.1483862
View Table of Contents: http://aip.scitation.org/toc/jcp/117/3
Published by the American Institute of Physics

Liquid xenon as an ideal probe for many-body effects in impulsive Raman scattering

Nienke H. Boeijenga
Theoretical Chemistry, Materials Science Centre, Rijksuniversiteit Groningen (RuG), Nijenborgh 4, 9747 AG Groningen, The Netherlands

Audrius Pugzlys
Ultrafast Laser Laboratory, Materials Science Centre, Rijksuniversiteit Groningen (RuG), Nijenborgh 4, 9747 AG Groningen, The Netherlands

Thomas I. C. Jansen and Jaap G. Snijders
Materials Science Centre, Rijksuniversiteit Groningen (RuG), Nijenborgh 4, 9747 AG Groningen, The Netherlands

Koos Duppen
Ultrafast Laser Laboratory, Materials Science Centre, Rijksuniversiteit Groningen (RuG), Nijenborgh 4, 9747 AG Groningen, The Netherlands

(Received 4 February 2002; accepted 16 April 2002)

The collision induced effects in the third-order Raman response of liquid xenon have been studied both experimentally and theoretically. The effect of electron cloud overlap on the polarizability of xenon dimers was studied using accurate time-dependent density functional theory calculations. The dimer polarizabilities were used to fit parameters in a direct reaction field model that can be generalized to condensed phase systems. This model was employed in molecular dynamics simulations in order to calculate the impulsive Raman response of liquid xenon. Excellent agreement is found between the shape of the calculated and the measured anisotropic part of the response. The shape of this response is little affected by the electron overlap effects, but the intensity is strongly influenced by it. The shape of the isotropic response is predicted to be strongly dependent on electron overlap effects. © *2002 American Institute of Physics.* [DOI: 10.1063/1.1483862]

I. INTRODUCTION

Atomic liquids are special because no intramolecular nuclear degrees of freedom are found in these systems. Therefore they provide a unique possibility of studying intermolecular interactions and motions, avoiding any contribution from or coupling to intramolecular degrees of freedom. Xenon is a noble gas that forms an atomic liquid at a relatively high temperature due to its large atomic mass and high polarizability. The latter effect not only gives rise to substantial interatomic coupling, but also to efficient interactions with optical fields.

Dynamic (inelastic) light scattering was employed by a number of groups to study the properties of liquid xenon.[1–3] In these experiments the information is obtained in the form of a (Raman) spectrum of interatomic motion. More recently, these frequency-domain spontaneous light scattering methods were complemented with a variety of time-domain techniques, based on stimulated light scattering of short (femtosecond) laser pulses.[4–15] Examples of these techniques are the (heterodyned) optical Kerr effect[4,5] and transient grating scattering.[6,7] These experiments probe the evolution of the first-order susceptibility (the macroscopic polarizability) after impulsive excitation of the system, allowing observation of the liquid motion in real time. The time-domain data of these third-order nonlinear optical experiments are related to the frequency-domain spectra from spontaneous light scattering by Fourier transformation.

Isolated xenon atoms have constant isotropic polarizabilities and therefore will not give rise to any Raman response. However, in the condensed phase many-body interactions lead to fluctuations in the susceptibility and hence a measurable Raman response. This makes atomic liquids such as liquid xenon excellent probes for studies of intermolecular interactions and motions. Some 15 years ago, Greene *et al.*[16] reported experimental results on the third-order Raman response of liquid xenon. Their limited time resolution allowed them to measure only the tail of the signal, which was found to be well described by exponential decay. This does not agree with the results of the earlier light scattering measurement by Gornall *et al.*,[1] which Bucaro and Litovitz[17] fitted to an analytical expression that shows t^{-n} decay in the long time limit. This expression was derived[17] using a model based on gas phase collisions.

In liquid xenon, two sources for the many-body effects, giving rise to a measurable Raman response exist: dipole-induced dipole interactions and the effect of electron cloud overlap. The first effect arises from the fact that two molecules in a macroscopic electric field do not only feel this macroscopic field, but also the local field generated by the dipoles induced on other molecules. The electron overlap effect arises when molecules come so close to each other that their electron clouds overlap, which will then also affect their polarizability. In most calculations of the third-order response till now, only the dipole-induced dipole effect has

been taken into account.[18–25] A few studies on molecules have used an atomic dipole-induced dipole (DID) model,[26,27] placing polarizabilities not only on the center-of-mass, but on all atoms, thereby introducing atomic structure and hence induced multipoles in an approximate manner. Recently, a study including both induced multipoles and electron overlap in the calculation of the third-order response of CS_2 was reported.[28] In that case it was shown that the effects of induced multipoles are more important than electron overlap. For xenon there are no induced multipole effects, so that only many-body interactions caused by the electron overlap effect and DID remains.

In this paper the many-body aspects of the third-order Raman response of liquid xenon are studied experimentally and by simulation. In Sec. II the theory behind the calculations is outlined. In Sec. III the experiments are presented. The simulations are described and compared to the experimental results in Sec. IV. Finally the conclusions are presented in Sec. V.

II. THEORY

The stimulated Raman response is governed by the third-order response function $\chi^{(3)}_{abcd}(t_1)$, where c and d denote the polarization directions of two initial laser fields that interact with the sample. After a delay t_1 the time evolution of the system is probed by a laser field with polarization direction b. This results in the emission of a signal field that is detected with polarization direction a. In the isotropic liquid phase two linear independent components of the third-order response exist.[29] These can be chosen to be the isotropic $[\chi^{(3)}_{zzmm}]$ and anisotropic $[\chi^{(3)}_{zxzx}]$ components, where m denotes an axis forming an angle, often denoted the magic angle, of 54.74° with the z-axis.

In the finite field method (FF),[20,28,30] the third-order response function is calculated by simulating the conditions of the experiment. The forces, due to the optical fields E_c and E_d are actually applied in the simulation. Motion is induced in the liquid by the linear response $\chi^{(1)}_{cd}$. The third-order response is determined by calculating the susceptibility $\chi^{(1)}_{ab;cd}(t)$, i.e., the linear response $\chi^{(1)}_{ab}$ at later time steps due to the action of the laser fields c and d. The procedure is repeated for numerous trajectories with different starting configurations producing sufficient statistical material. The background noise $\chi^{(1)}_{ab;00}(t)$, from calculations without the applied forces is subtracted to improve accuracy. For laser fields with duration Δt and a number density N in the sample the response function is given by

$$\chi^{(3)}_{abcd}(t)=\frac{\chi^{(1)}_{ab;cd}(t)-\chi^{(1)}_{ab;00}(t)}{4\pi\epsilon_0 NE_cE_d\Delta t}. \tag{1}$$

The FF method has been shown to be equally good as the more conventional time-correlation function method, when the third-order response function is calculated.[30] In terms of calculating costs and possibilities it is superior to this method, when higher order response functions such as $\chi^{(5)}_{abcdef}(t_1,t_2)$ are evaluated.[20,30]

Bucaro and Litovitz derived an expression for the spontaneous Raman scattering (frequency domain) due to interaction induced effects, based on an atomic collision model.[17] This is related by a Fourier transform to the stimulated third-order Raman response (time domain),

$$\chi^{(3)}(t)\propto\frac{\tau_C^n\sin(n\tan^{-1}(t/\tau_C))}{(t^2+\tau_C^2)^{n/2}}, \tag{2}$$

where τ_C is the collision time and n is related to the character of the interaction. The expression has been used by several authors to fit experimental spectra.[14,17,28] One should be very careful doing this, since it was derived for collisions of isolated dimers with zero impact parameter.[17] The frequency domain response was originally given as

$$\chi^{(3)}(\omega)\propto\omega^{2[(m-7)/7]}\exp(-\omega/\omega_0), \tag{3}$$

where ω_0 is the inverse of τ_C and $2[(m-7)/7]$ is equal to $n-1$ $(m=[7n+7]/2)$. In the paper by Bucaro and Litovitz[17] the time constant τ_C was related to the interaction parameters in an approximate way,

$$\tau_C\approx\tfrac{1}{6}\pi r_0(\mu/kT)^{1/2}[1-(2/\pi)\tan^{-1}(2\epsilon/kT)^{1/2}]. \tag{4}$$

Here ϵ and r_0 are the potential depth and distance in a supposed Lennard-Jones potential and μ is the reduced mass. The constant m was related to the polarizability dependence on the interatomic distance r,

$$\alpha(r)-\alpha(\infty)\propto r^{-m}. \tag{5}$$

We will use time-dependent density functional theory (TDDFT) (Ref. 31) to calculate the microscopic counterpart of the susceptibility, i.e., the polarizability. Since this method is far too time consuming to be used to calculate the polarizability of large numbers of molecules, the more efficient but approximated direct reaction field (DRF) model[32–36] is employed for this purpose. The parameters of this model are optimized to reproduce the TDDFT results for dimers. The DRF model is then generalized to calculate the first-order susceptibility of MD simulation boxes containing hundreds of atoms.

In the DRF model,[32–36] the conventional dipole field tensor that describes the dipole induced-dipole interaction, is replaced by a modified one that also takes the effect of overlapping electron clouds into account. The first-order susceptibilities $\chi^{(1)}$ in Eq. (1) can be found by solving a linear set of equations,[18–20,32,34,35]

$$\chi^{(1)}=\frac{1}{V}\sum_p\Pi_p, \tag{6}$$

$$\sum_p B_{qp}\Pi_p=L, \tag{7}$$

$$B_{qp}\equiv\alpha_q^{-1}\delta_{qp}-\mathcal{T}_{qp}(1-\delta_{qp}), \tag{8}$$

where Π_p is an effective polarizability on atom p, α_p is the isolated atom polarizability, V the volume, and L is the Lorentz factor. The modified dipole field tensor $\mathcal{T}_{pq}$ is given by

$$\mathcal{T}_{pq}=\frac{3f^T_{pq}(\hat{r}_{pq}:\hat{r}_{pq})-f^E_{pq}}{r^3_{pq}}. \tag{9}$$

FIG. 1. Dimer rotation and dimer collision. Rotation only changes the anisotropic polarizability. Collision changes both the isotropic and the anisotropic polarizability.

Here $\mathbf{r}_{pq}$ is the distance vector between the interacting dipoles. The screening functions f_{pq}^{T} and f_{pq}^{E} take the effect of overlapping charge densities into account. In the DID limit these factors are one. In the exponential density model they are[32,34]

$$f_{pq}^{E}=1-(\tfrac{1}{2}\nu_{pq}^{2}+\nu_{pq}+1)\exp(-\nu_{pq}), \tag{10}$$

$$f_{pq}^{T}=f_{pq}^{E}-\frac{\nu_{pq}^{3}}{6}\exp(-\nu_{pq}), \tag{11}$$

$$\nu_{pq}=\frac{\mathbf{a}r_{pq}}{(\alpha_{p}\alpha_{q})^{1/6}}. \tag{12}$$

The empiric screening factor **a**, and the atomic polarizability α are usually optimized to give as good a description of the molecular polarizability as possible for a wide variety of molecules.[34] In this work on liquid xenon the model will be optimized to reproduce the TDDFT result for the polarizability of a xenon dimer. Subsequently, the DRF approach was used to calculate the first-order susceptibility, in the same manner as described in our paper on CS_2.[28]

In Fig. 1 the two possible interatomic motions in a dimer are sketched, i.e., a dimer rotation and a dimer collision with zero impact parameter. The dimer rotation will not change the isotropic polarizability of the dimer and hence will only contribute to the anisotropic response. The head on collisions will change both the anisotropic and the isotropic polarizability and will therefore give a contribution to both components of the optical response.

III. EXPERIMENTS

The anisotropic Raman response of xenon was measured in an OHD-Kerr experiment, as proposed by McMorrow and Lotshaw.[13] Briefly, we used a Ti:sapphire oscillator (Mai Tai, Spectra-Physics) delivering ~70 fs pulses centered around 800 nm at an 82 MHz repetition rate. The output of the laser after precompression in a doublepass compressor based on two fused silica prisms, was ~7 nJ per pulse. This output was split into pump and probe beams with a ratio of 10:1, respectively. The probe pulse was variably delayed by a computer controlled delay stage. The pump and probe beams were polarized at 45° with respect to each other and were focused into a sample by using a spherical mirror of $r=25$ cm. The necessary pump and probe polarization orientations were set by 3 mm thick Glan–Taylor polarizers and a $\lambda/2$ plate in the pump beam. The energy of the excitation pulses in the sample place did not exceed 2 nJ per pulse. The 90° out-of-phase local oscillator field was generated by insertion of a $\lambda/4$ plate in the probe beam and detuning of the probe polarizer by ~1.5°. By measuring the crosscorrelation function of the pump and probe beams in a 20 μm BBO crystal and applying a deconvolution procedure in frequency domain[37,38] the inertial nuclear contributions to the transients were separated from distortions introduced by the instantaneous electronic response. The FWHM of the electronic response was measured to be 120 fs.

TABLE I. Exponents of the diffuse functions added to the ADF Xe V ZORA basis set with specific n power dependence in the radial part and spherical harmonic behavior.

s-functions		*p*-functions		*d*-functions		*f*-functions	
n	exponent	n	exponent	n	exponent	n	exponent
5	1.2	4	3.2	3	6.2	4	1.3
	0.8		2.133	4	2.1		0.889
	0.533	5	0.81		1.4		0.0.593
	0.355		0.506		0.933		0.395
			0.316		0.622		
			0.198		0.415		
			0.123				

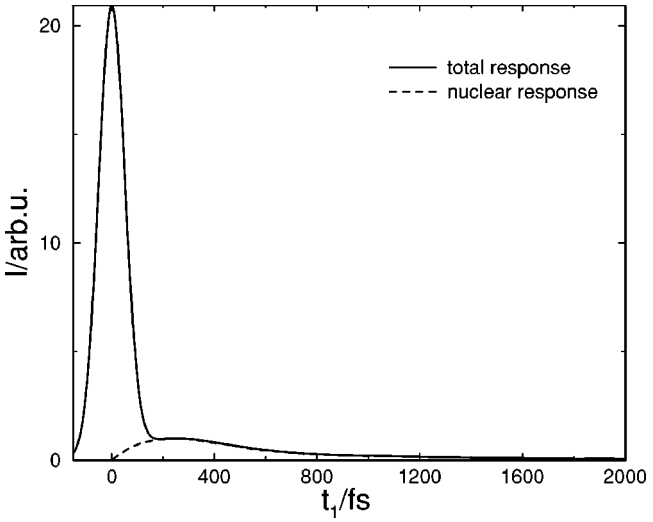

FIG. 2. The measured anisotropic third-order Raman response (solid line), together with the anisotropic deconvoluted nuclear response (dashed line), obtained by deconvoluting the electronic response.

Liquid xenon was condensed into the 2 cm path length sample space of a liquid nitrogen flow cryostat (Oxford DN1714) from 99.997% purity xenon gas. Experiments were performed at a temperature of 164 ± 0.5 K. The temperature of the liquid xenon was controlled by employing an active feedback device and monitored during the experiments. At 1 bar the melting point of xenon is 161.25 K and the boiling point is 166.15 K.[39] The dependence of the OHD Kerr response on temperature was investigated over this range, but was found to be almost negligible.

The experimental result of a OHD Kerr effect experiment at 164 K is shown in Fig. (2). It is clear that the nuclear contribution to this signal is rather small compared to the electronic one. When the latter is removed by Fourier deconvolution,[37,38] the dashed trace is obtained. It is proportional to the anisotropic component $\chi_{zxzx}^{(3)}$ of the third-order

TABLE II. Number of fit functions added to the ADF Xe V ZORA basis set with specific n power dependence in the radial part and spherical harmonic behavior.

s-functions		*p*-functions		*d*-functions		*f*- functions		*d*-functions	
n	No. fit f	n	No. fit f	n	No. fit f	n	No. fit f	n	No. fit f
1	6	1		1		1		1	
2	2	2	1	2		2		2	
3	2	3	1	3	2	3		3	
4	2	4	3	4	3	4	3	4	
5	3	5	4	5	3	5	4	5	3
6	4	6	4	6	5	6	5	6	4
7	4	7	5	7	5	7	7	7	5
8	5	8	6	8	6	8	8	8	7
9	6	9	7	9	7				

Raman response of liquid xenon. This result will be compared to simulations below.

IV. SIMULATIONS

The frequency dependent polarizability of the xenon atom and dimer were calculated with the Time Dependent Density Functional Theory (TDDFT), using the Amsterdam Density Functional (ADF) (Refs. 31, 40–43) package. The basis set used is a standard ADF ZORA all electron triple zeta basis set with polarization (called ''ZORA V all electron'') to which diffuse functions have been added (Table I). This is required for calculations of the polarizability, where displacement of weakly bound electrons in the diffuse region gives a significant contribution. The set of fit-functions was also expanded (Table II) and new coefficients were found with the program GENFIT, which is part of the ADF distribution. The LB94 (Ref. 44) potential with proper asymptotic behavior in the diffuse region was used in these calculations. This potential was shown to give good results for the polarizability of a large series of molecules.[45] Relativistic effects are expected to be of some importance since xenon is a rather heavy element.[46–48] The scaled ZORA approach,[49–52] implemented in the ADF, was used to take the scalar relativistic effects into account. The value for the atomic polarizability of xenon at a frequency of 0.0934 a.u. was found to be 4.177 Å, deviating only 1% from experiment.[2] Typical absolute deviations in such polarizability calculations, using the same method, are 3.6%.[45]

In order to compare the relative importance of the DID and collisional many-body effects on the optical response, simulations were performed where only the DID effect was incorporated, and simulations in which both effects were taken into account by the DRF method. In both the DID and DRF calculations the TDDFT single atom polarizability is taken as the starting point. All polarizabilities were calculated at a frequency of 0.076 071 a.u. (598.96 nm), at which frequency the calculated atomic polarizability is 4.116 Å. The DRF model was optimized to the TDDFT calculations with the POLAR program.[33] In the optimization the xenon polarizabilities were kept fixed at the calculated single atom value of 4.116 Å. The screening factor **a**, which takes account of the electron cloud overlap, was optimized to dimer calculations with interatomic distances from 3 to 8 Å. It was found to be 2.587 85, which is somewhat higher than the value of 1.9088 found in the optimization of a wide range of molecules.[33] The dimer polarizabilities, found with the DID and DRF models, as well as with TDDFT, are shown in Fig. 3. At an interatomic distance of 4.3 Å, where the first solvation shell peaks, the value for the polarizability α_{zz} obtained with the DID model is 1.2% too high compared to the TDDFT result. At the closest interatomic distance found in the simulations, 3.55 Å, the DID polarizability α_{zz} is 5.5% too high. The slope of the DID polarizability vs interatomic distance is much steeper than the slope of the TDDFT curve. The optimized DRF model on the other hand shows excellent agreement with the TDDFT results.

MD simulations were performed with GROMACS 1.6.[53] The temperature was set to 163 K and the pressure to 1 bar. The calculation box contains 256 atoms. The Lennard-Jones coefficients for the simulations were obtained by a fit to the xenon potential energy curve recently calculated by Faas *et al.*[47] The coefficients are $C_6 = 3.379 \times 10^{-2}$ kJ nm^6/mol and $C_{12} = 1.380 \times 10^{-4}$ kJ nm^{12}/mol. The calculated MD density of 2.9 kg/l shows good agreement with the literature value[54] of 2.969 kg/l, measured at 161.36 K and 0.8203 bar.

The third-order Raman response calculated with the DID model and the DRF model are compared in Fig. 4. The first striking feature is that the isotropic response is very small

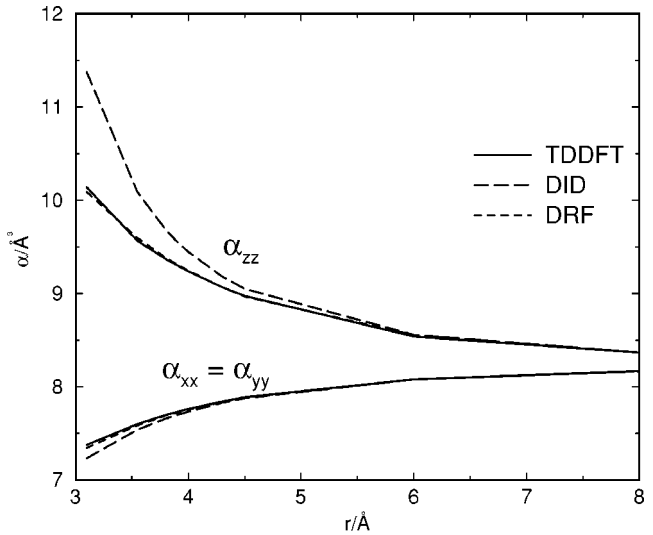

FIG. 3. Dimer polarizabilities calculated parallel and perpendicular to the interatomic (x) axis.

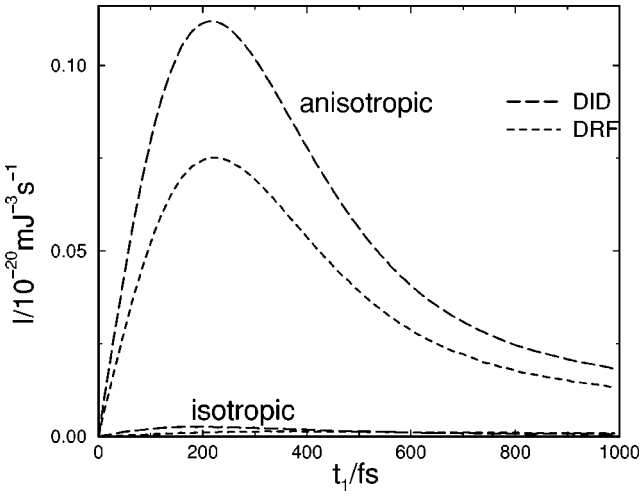

FIG. 4. The isotropic and anisotropic third-order responses calculated with the DID and DRF model.

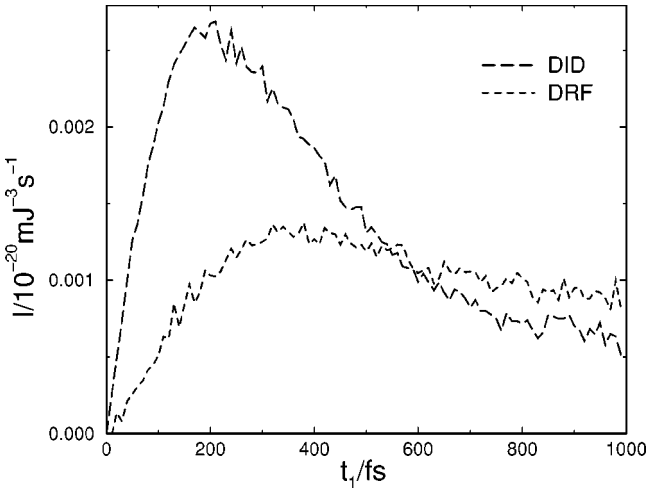

FIG. 5. Comparison of the third-order isotropic responses calculated with the DID and DRF models.

compared to the anisotropic response, as was expected (see Sec. II). The isotropic response is almost fifty times smaller than the anisotropic response. The second noticeable observation is the fact that the anisotropic responses, calculated with the DID and DRF models, have the same overall shape but very different intensities. Including electron overlap reduces the signal intensity by a factor of 1.5.

In Fig. 5 the calculated isotropic responses are compared. Because of the small intensities of these signals, the signal to noise ratio is rather small. It is clear however that the shapes of the isotropic responses of the two models are not the same. Both the isotropic and anisotropic responses have been fitted to the atomic collision model expression [Eq. (2)] given in Sec. II. The values for the respective constants are shown in Table III. For comparison, the value for the time constant τ_c was also calculated with the thermodynamic expression Eq. (4). The time constant τ_c of the isotropic DRF result comes closest to τ_c from expression (4). This is to be expected since the phenomenological model was derived for atomic collisions with zero impact parameter. The isotropic response indeed depends on these collisions but not on the dimer rotations.

The normalized anisotropic DRF and DID nuclear responses both show excellent agreement with the measured response (see Fig. 6). However, the maximum occurs somewhat earlier in the calculated curves than in the experimental curve. The difference is very small, but the DRF result seems to be slightly closer to the experiment, especially in the tail.

V. CONCLUSIONS

Liquid xenon was studied to investigate the effects of overlapping electron clouds and dipole induced-dipole interactions on the optical response. Xenon is eminently suited for this purpose, since the single atoms do not generate a Raman signal and all observed response is therefore due to many-body effects. Experimental results on impulsive anisotropic scattering were obtained by OHD-Kerr experiments. MD simulations were performed using the DRF model for the optical interactions, optimized against TDDFT calculations of the polarizability of dimers.

By comparing the DRF results to a model in which only DID effects are taken into account, it was shown that electron overlap effects are quite important, also at distances typically found in MD simulations. The electron overlap effect is seen to lower the intensity of the response. In the anisotropic case the shape of the response was only slightly affected by the electron overlap effect, whereas for the isotropic response the shape was found to be quite sensitive to the electron overlap effect.

Both the DID and DRF calculated responses agree excellently with the shape of the measured anisotropic response, even though the DRF result is slightly closer to the experimental one. The small deviations observed can originate both from experimental factors such as small errors introduced in the deconvolution procedure and from approximations done in the calculations such as the use of a Lennard-Jones potential. The fact that the maximum of the

TABLE III. Values for τ_c, n, and m found from fits to calculations and experiment. I_C is the intensity.

	Anisotropic			Isotropic	
	Expt.	DID	DRF	DID	DRF
I_C	⋯	0.173	0.116	0.00442	0.00242
τ_c/fs	342	353	359	267	427
n	1.72	1.92	1.90	1.52	1.13
m	9.5	10	10	8.8	7.5

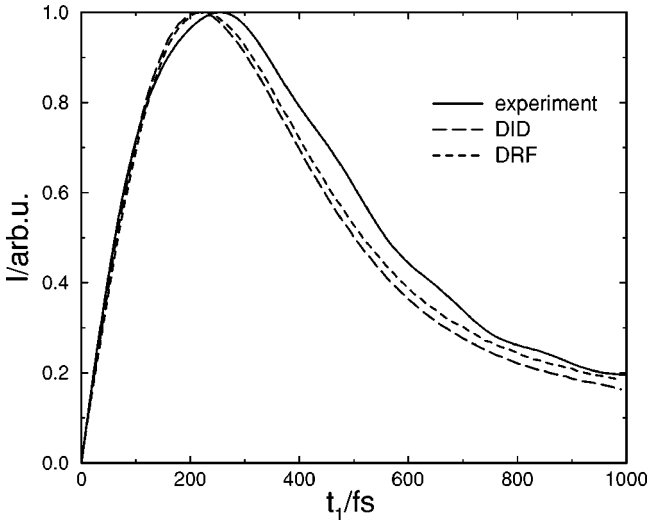

FIG. 6. Comparison of the normalized calculated anisotropic third-order Raman response with the deconvoluted anisotropic nuclear experimental response.

calculated signal occurs at a somewhat shorter timescale than the experimental one, might in that case be indicative of too high intermolecular frequencies, i.e., of too steep potentials.

It would be interesting if it was possible to detect the very weak isotropic response experimentally, since the shape was found to be very sensitive to the electron overlap effect in the calculations. Recent developments in the spectroscopical techniques[55] might make such measurements possible. Such attempts are now in progress.

Both the calculated and experimental response functions could be fitted quite well to the expression in Eq. (2). The fit constants agree reasonably well with the theory of Bucaro and Litovitz,[17] but we believe that one should be cautious interpreting the liquid response with a model based on collisions in vacuum with zero impact parameter.

The importance of electron overlap effects will probably also be observable in the fifth-order response of xenon that has been investigated theoretically by others.[56,57] Supposing that the difficulties of the experimental techniques,[58,59] used to detect the fifth-order signals, can be overcome, the fifth-order response might provide other important clues to the importance of the electron overlap effects.

[1] W. S. Gornall, H. E. Howard-Lock, and B. P. Stoicheff, Phys. Rev. A **1**, 1288 (1970).
[2] L. Frommhold, K. H. Hong, and M. H. Proffitt, Mol. Phys. **35**, 691 (1978).
[3] P. A. Fleury, J. M. Worlock, and H. L. Carter, Phys. Rev. Lett. **30**, 591 (1973).
[4] T. Steffen, N. A. C. M. Meinders, and K. Duppen, J. Phys. Chem. A **102**, 4213 (1998).
[5] D. McMorrow, N. Thantu, J. S. Melinger, S. K. Kim, and W. T. Lotshaw, J. Phys. Chem. **100**, 10389 (1996).
[6] S. Ruhman, L. R. Williams, A. G. Joly, and K. A. Nelson, J. Phys. Chem. **91**, 2237 (1987).
[7] A. Waldman, U. Banin, E. Rabani, and S. Ruhman, J. Phys. Chem. **96**, 10840 (1992).
[8] C. Kalpouzos, D. McMorrow, W. T. Lotshaw, and G. A. Kenney-Wallace, Chem. Phys. Lett. **150**, 138 (1988).
[9] C. Kalpouzos, D. McMorrow, W. T. Lotshaw, and G. A. Kenney-Wallace, Chem. Phys. Lett. **155**, 240 (1989).
[10] M. Neelakandan, D. Pant, and E. L. Quitevis, Chem. Phys. Lett. **265**, 283 (1997).
[11] A. Idrissi, P. Bartolini, M. Ricci, and R. Righini, J. Chem. Phys. **114**, 6774 (2001).
[12] A. Idrissi, M. Ricci, P. Bartolini, and R. Righini, J. Chem. Phys. **111**, 4148 (1999).
[13] D. McMorrow, W. T. Lotshaw, and G. A. Kenney-Wallace, IEEE J. Quantum Electron. **24**, 443 (1988).
[14] T. Hattori and T. Kobayashi, J. Chem. Phys. **94**, 3332 (1991).
[15] D. McMorrow and W. T. Lotshaw, Chem. Phys. Lett. **201**, 369 (1993).
[16] B. I. Greene, P. A. Fleury, H. L. Carter, Jr., and R. C. Farrow, Phys. Rev. A **29**, 271 (1984).
[17] J. A. Bucaro and T. A. Litovitz, J. Chem. Phys. **54**, 3846 (1971).
[18] L. C. Geiger and B. M. Ladanyi, J. Chem. Phys. **87**, 191 (1987).
[19] L. C. Geiger and B. M. Ladanyi, Chem. Phys. Lett. **159**, 413 (1989).
[20] T. l. C. Jansen, J. G. Snijders, and K. Duppen, J. Chem. Phys. **114**, 10910 (2001).
[21] K. Kiyohara, K. Kamada, and K. Ohta, J. Chem. Phys. **112**, 6338 (2000).
[22] B. M. Ladanyi, Chem. Phys. Lett. **121**, 351 (1985).
[23] P. A. Madden, ''Interaction-induced, subpicosecond phenomena in liquids,'' in *Ultrafast Phenomena*, edited by D. H. Auston and K. B. Eisenthal (Springer, Berlin, 1985), Vol. IV, p. 244.
[24] H. Stassen, Th. Dorfmüller, and B. M. Ladanyi, J. Chem. Phys. **100**, 6318 (1994).
[25] H. Stassen and W. A. Steele, J. Chem. Phys. **110**, 7382 (1999).
[26] X. Ji, H. Alhborn, B. Space, P. B. Moore, Y. Zhou, S. Constantine, and L. D. Ziegler, J. Chem. Phys. **112**, 4186 (2000).
[27] R. L. Murry, J. T. Fourkas, and T. Keyes, J. Chem. Phys. **109**, 2814 (1998).
[28] T. l. C. Jansen, M. Swart, L. Jensen, P. Th. van Duijnen, J. G. Snijders, and K. Duppen, J. Chem. Phys. **116**, 3277 (2002).
[29] A. Tokmakoff, J. Chem. Phys. **105**, 1 (1996).
[30] T. l. C. Jansen, J. G. Snijders, and K. Duppen, J. Chem. Phys. **113**, 307 (2000).
[31] S. J. A. van Gisbergen, J. G. Snijders, and E. J. Baerends, Comput. Phys. Commun. **118**, 119 (1999).
[32] B. T. Thole, Chem. Phys. **59**, 341 (1981).
[33] P. Th. van Duijnen and M. Swart, J. Phys. Chem. A **102**, 2399 (1998).
[34] M. Swart, P. Th. van Duijnen, and J. G. Snijders, J. Mol. Struct.: THEOCHEM **458**, 11 (1999).
[35] C. J. F. Böttcher and P. Bordewijk, *Theory of Electric Polarization* (Elsevier, Amsterdam, 1978).
[36] A. J. Stone, ''The theory of intermolecular forces,'' Vol. 32 in *International Series of Monographs on Chemistry* (Oxford University Press, Oxford, 1996).
[37] D. McMorrow and W. T. Lotshaw, Chem. Phys. Lett. **174**, 85 (1990).
[38] D. McMorrow and W. T. Lotshaw, J. Phys. Chem. **95**, 10395 (1991).
[39] *CRC Handbook of Chemistry and Physics*, 63rd ed., edited by R. C. Weast (CRC, Boca Raton, 1983–1984).
[40] E. J. Baerends, D. E. Ellis, and P. Ros, Chem. Phys. **2**, 41 (1973).
[41] G. te Velde and E. J. Baerends, J. Comput. Phys. **99**, 41 (1992).
[42] S. H. Vosko, L. Wilk, and M. Nusair, Can. J. Phys. **58**, 1200 (1980).
[43] G. te Velde, F. M. Bickelhaupt, E. J. Baerends, C. Fonseca Guerra, S. J. A. van Gisbergen, J. G. Snijders, and T. Ziegler, J. Comput. Chem. **22**, 931 (2001).
[44] R. van Leeuwen and E. J. Baerends, Phys. Rev. A **49**, 2421 (1994).
[45] S. J. A. van Gisbergen, F. Kootstra, P. R. T. Schipper, O. V. Gritsenko, J. G. Snijders, and E. J. Baerends, Phys. Rev. A **57**, 2556 (1998).
[46] E. Radzio and J. Andzelm, J. Comput. Chem. **8**, 117 (1987).
[47] S. Faas, J. H. van Lenthe, and J. G. Snijders, Mol. Phys. **98**, 1467 (2000).
[48] N. Runeberg and P. Pyykkö, Int. J. Quantum Chem. **66**, 131 (1998).
[49] C. H. Change, M. Pelissier, and P. H. Durand, Phys. Scr. **34**, 394 (1986).
[50] J. L. Heully, I. Lindgren, E. Lindroth, S. Lundquist, and A. M. Mårtensson-Pendrill, J. Phys. B **19**, 2799 (1986).
[51] E. van Lenthe, E. J. Baerends, and J. G. Snijders, J. Chem. Phys. **99**, 4597 (1993).
[52] E. van Lenthe, E. J. Baerends, and J. G. Snijders, J. Chem. Phys. **101**, 1272 (1994).
[53] H. J. C. Berendsen, D. van der Spoel, and R. van Drunen, Comput. Phys. Commun. **91**, 43 (1995).
[54] C. Chui and F. B. Canfield, Trans. Faraday Soc. **67**, 2933 (1971).

[55] Q.-H. Xu, Y.-Z. Ma, and G. R. Fleming, Chem. Phys. Lett. **338**, 254 (2001).
[56] A. Ma and R. M. Stratt, Phys. Rev. Lett. **85**, 1004 (2000).
[57] R. A. Denny and D. R. Reichman, Phys. Rev. E **63**, 065101 (2001).
[58] D. A. Blank, L. J. Kaufman, and G. R. Fleming, J. Chem. Phys. **111**, 3105 (1999).
[59] D. A. Blank, L. J. Kaufman, and G. R. Fleming, J. Chem. Phys. **113**, 771 (2000).